Electronic Supplementary Material (ESI) for Journal of Materials Chemistry A.
This journal is © The Royal Society of Chemistry 2021

Supporting Information

Tuning $Na_3Hf_2Si_2PO_{12}$ electrolyte surfaces by metal coating for high-rate and long cycle life solid-state sodium ion batteries

Shen Cai,[a] Haoqing Tian,[a] Jiahui Liu,[a] Shan Liu,[a*] Lei Dai,[a] Junjie Xu,[b] Lingxin Kong,[b*] Ling Wang[a*]

[a] School of Chemical Engineering, North China University of Science and Technology, Tangshan, 063009, China. Email: sliu@ncst.edu.cn, tswling@126.com

[b] Faculty of Metallurgical and Energy Engineering, Kunming University of Science and Technology, No. 253, Xuefu road, Kunming 650093, China. Email: kkmust@126.com

Experimental Section

NASICON-type $Na_3Hf_2Si_2PO_{12}$ (NHSP) electrolyte fabrication: First, the NHSP powder was prepared by a solid-state reaction method. A proper ratio of Na_2CO_3 (99.8%), HfO_2 (99.8%), SiO_2 (99.9%), and $NH_4H_2PO_4$ (99.9%) were ball-milled with ethanol as dispersant for 48 h. The mixture was blown dry and sintered at 900 °C for 8 h. The obtained powder was pressed into pellets with a diameter of 12 mm and the thickness of 1 mm, and sintered at 1250 °C for 16 h. The bare NHSP pellets were obtained after polishing and drying.

Pb Layer Coating: The Pb layer on the surface of NHSP was realized by vacuum arc ion plating. The chamber vacuum before sputtering was about 1.0×10^{-4} Pa and the current is 20 mA. The NHSP pellets were carefully polished before sputtering and Pb was sputtered on both sides of NHSP for symmetric batteries and on one side for full cells. The thickness of Pb layer was about 50 nm after sputtering for 500 s.

Structural and Morphology Characterizations: Morphologies of samples were characterized by scanning electron microscope (SEM, Hitachi S4800) coupled with EDS. The XRD patterns were tested by Riguka D/max 2500/PC diffractmeter using Cu Kα radiation (λ = 1.5418 Å), the angle range is 10-90° (2θ). The impedance of batteries was obtained by EIS in the frequency range of 10 kHz to 1 Hz with a voltage amplitude of 10 mV. The charge-discharge data were obtained on a Land 2001A battery testing system. The Tafel data were conducted by a CHI660E electrochemical workstation. The conductivity and Na^+ migration number of the electrolyte were measured by the alternating impedance method (EIS, IM6 electrochemical workstation, German Global Analysis and Testing Instrument Co LTD.) at the temperature range of 30-300 °C.

Batteries construction and testing: First, in order to guarantee a sufficient reaction between the metal Na and the Pb layer, the Na metal surface was scraped to remove

the oxide layer and after that, the clean sodium sheet was attached to the Pb-coated NHSP pellets to assemble the batteries. Na|Pb-NHSP-Pb|Na symmetric batteries and Na|Pb-NHSP|$Na_3V_2(PO_4)_3$ full cells were assembled. The $Na_3V_2(PO_4)_3$ cathode included 70 wt% $Na_3V_2(PO_4)_3$ sample, 20 wt% Super P, and 10 wt% PVDF on an Al foil. After drying overnight in a vacuum oven, cut it into 10 mm diameter plates with mass loading was around 1.0 mg cm^{-2}. In addition, 20 μL $NaClO_4$ electrolyte was used between NHSP pellets and $Na_3V_2(PO_4)_3$ cathodes. All the battery assembly process was carried out in an Ar-filled glovebox.

Computational details: The energy barrier for were conducted with Vienna ab initio simulation package code in density functional theory. The generalized gradient approximation (GAA) of Perdew-Burke-Ernzerhof (PBE) was functioned with a cut-off energy of 370 eV. The parameter of energy and force convergence was set as 10^{-5} eV and 0.02 eV $Å^{-1}$, respectively. For structure optimization, the Monkhorst-Pack k points was set as 3 × 3 × 1. To investigate the ionic conductivity transport process in Na_xPb, sodium through vacancy mechanism in $Na_{15}Pb_4$ was simulated through Climbing Image NEB (cNEB) method.[1] The migration path and diffusion energy barriers are obtained.

Calculation of thermodynamics: According Miedema model, the calculation formula of i-j system is as follows.

$$\Delta H_{ij} = x_i(2P\frac{x_i V_i^{2/3}}{x_i V_i^{2/3} + x_j V_j^{2/3}}\left\{1 + \sigma\left[\frac{x_i V_i^{2/3} x_j V_j^{2/3}}{(x_i V_i^{2/3} + x_j V_j^{2/3})^2}\right]^2\right\} \times \frac{9.4\left(n_{ws}{}_i^{1/3} - n_{ws}{}_j^{1/3}\right)^2 - \left(\Phi_i - \Phi_j\right)^2 - a\left(\frac{r}{p}\right)_{ij}}{n_{ws}{}_i^{-1/3} + n_{ws}{}_j^{-1/3}} + \Delta H^{trans}) \quad (1)$$

$$\Delta S_{ij}^E = \frac{1}{14}\Delta H_{ij}\left(\frac{1}{T_{mi}} + \frac{1}{T_{mj}}\right) \quad (2)$$

$$\Delta G_{ij}^{E} = \left[1 - \frac{1}{14} T \left(\frac{1}{T_{mi}} + \frac{1}{T_{mj}}\right)\right] \Delta H_{ij} \quad (3)$$

$$ln\gamma_i = \frac{a_{ij}\Delta H_{ij}}{RT}\left[1 + x_j\left[\frac{1}{x_i} - \frac{1}{x_j} - \frac{\mu_i(\phi_i - \phi_j)}{[1 + \mu_i x_j(\phi_i - \phi_j)]} + \frac{\mu_j(\phi_j - \phi_i)}{[1 + \mu_j x_i(\phi_j - \phi_i)]} - \frac{\frac{2}{V_i^3}[1 + \mu_i}{x_i V} \quad (4)$$

Herein, ΔH_{ij} is the enthalpy of formation; ΔS_{ij}^{E} is the excess entropy; ΔG_{ij}^{E} is the excess Gibbs free energy; γ_i is the activity coefficient of component i; x_i, x_j are the molar fractions of component i and j respectively; σ is an empirical parameter: it takes the value 0 for disordered alloys and the value 8 for ordered alloys; μ_i is the experimental volume shrinkage parameter for component i: it takes the value of 0.14 for alkali metals, 0.10 for alkaline earth metals or other bivalent metals, 0.07 for trivalent and precious metals, and 0.04 for other metals; V_i, V_j are the molar volumes of component i and j respectively; Φ_i, Φ_j are the electronegativity of component i and j respectively; n_{wsi}, n_{wsj} are the electron densities of component i and j respectively; The values of V, Φ, n_{ws} are available in Table S1; P is an empirical parameter: in the Miedema model, the metals are classified as class α (mainly transition metals) and class β (mainly non-transition metals); for components i and j, the value of P takes 10.70 if both belong to class α; the value of P takes 14.20 if both belong to class β; the value of P takes 12.35 if the component belong to class α and β respectively, and the classification can be checked in Table S2; $\left(\frac{r}{p}\right)_{ij} = \left(\frac{r}{p}\right)_i \times \left(\frac{r}{p}\right)_j$ if the component belongs to class α and β respectively, $\left(\frac{r}{p}\right)_{ij} = 0$ if both belong to the same class. The value of r/p is available in Table S2. a is a parameter that takes the value of 0.73 for liquid alloys and 1 for solid alloys; ΔH^{trans} is the enthalpy of phase change due to the entropy increase caused by the phase change in the system, and it is too small to be neglected in qualitative calculations; T_{mi} and T_{mj} are the melting points of i and j

respectively.

Table S1. The values of Φ, n_{ws}, and V for different elements.

H 5.20 3.38 1.70														
Li 2.85 0.94 13.00	Be 5.05 4.66 4.90	M ϕ n_{WS} V	Symbol in volt in density units in cm^3								Be 5.05 4.66 4.90	B 5.30 5.36 4.70	C 6.24 5.55 3.26	N 6.86 4.49 4.10
Na 2.70 0.55 23.78	Mg 3.45 1.60 14.00										Mg 3.45 1.60 14.00	Al 4.20 2.70 10.00	Si 4.70 3.38 8.60	P 5.55 4.49 8.60
K 2.25 0.27 45.63	Ca 2.55 0.75 26.20	Sc 3.25 2.05 15.03	Ti 3.80 3.51 10.58	V 4.25 4.41 8.36	Cr 4.65 5.18 7.23	Mn 4.45 4.17 7.35	Fe 4.93 5.55 7.09	Co 5.10 5.36 6.70	Ni 5.20 5.36 6.60	Cu 4.45 3.18 7.12	Zn 4.10 2.30 9.17	Ga 4.10 2.25 11.82	Ge 4.55 2.57 9.87	As 4.80 3.00 11.85
Rb 2.10 0.22 56.07	Sr 2.40 0.59 33.93	Y 3.20 1.77 19.90	Zr 3.45 2.80 14.00	Nb 4.05 4.41 10.80	Mo 4.65 5.55 9.40	Tc 5.30 5.93 8.64	Ru 5.40 6.13 8.20	Rh 5.40 5.45 8.30	Pd 5.45 4.66 8.90	Ag 4.35 2.52 10.25	Cd 4.05 1.91 13.00	In 3.90 1.60 15.75	Sn 4.15 1.90 16.30	Sb 4.40 2.00 16.95
Cs 1.95 0.17 69.23	Ba 2.32 0.53 38.10	La 3.17 1.64 22.55	Hf 3.60 3.05 13.45	Ta 4.05 4.33 10.81	W 4.80 5.93 9.55	Re 5.20 6.33 8.85	Os 5.40 6.33 8.45	Ir 5.55 6.13 8.52	Pt 5.65 5.64 9.10	Au 5.15 3.87 10.20	Hg 4.20 1.91 14.08	Tl 3.90 1.40 17.23	Pb 4.10 1.52 18.28	Bi 4.15 1.56 19.32
	Ce^{3+} 3.18 1.69 21.62	Pr 3.19 1.73 20.79	Nd 3.19 1.73 20.58	Pm 3.19 1.77 20.25	Sm 3.20 1.77 20.01	Eu^{3+} 3.20 1.77 19.97	Gd 3.20 1.77 19.90	Tb 3.21 1.82 19.32	Dy 3.21 1.82 19.00	Ho 3.22 1.82 18.76	Er 3.22 1.86 18.45	Tm 3.22 1.86 18.12	Yb^{3+} 3.22 1.86 17.97	Lu 3.22 1.91 17.77
			Th 3.30 2.10 19.80	Pa	U 3.90 3.44 13.15	Np	Pu 3.80 2.99 12.06							

Table S2. The classification of metals and the values of r/p for different elements.

class α											class β			
IIA	Transition metals,IIIA-VIIIA								IB		Be 0.4	B 1.9	C 2.1	N 2.3
Ca 0.4	Sc 0.7	Ti 1.0	V 1.0	Cr 1.0	Mn 1.0	Fe 1.0	Co 1.0	Ni 1.0	Cu 0.3		Mg 0.4	Al 1.9	Si 2.1	
Sr 0.4	Y 0.7	Zr 1.0	Nb 1.0	Mo 1.0	Tc 1.0	Ru 1.0	Rh 1.0	Pd 1.0	Ag 0.15		Zn 1.4	Ga 1.9	Ge 2.1	As 2.3
Ba 0.4	La 0.7	Hf 1.0	Ta 1.0	W 1.0	Re 1.0	Os 1.0	Ir 1.0	Pt 1.0	Au 0.3		Cd 1.4	In 1.9	Sn 2.1	Sb 2.3
	Th 0.7	U 1.0	Pu 1.0								Hg 1.4	Tl 1.9	Pb 2.1	Bi 2.3

Table S3. Calculated values of $\Delta H_{\text{Na-Pb}}$, $\Delta S^{E}_{\text{Na-Pb}}$, $\Delta G^{E}_{\text{Na-Pb}}$, γ_{Na} and γ_{Pb} of Na-Pb alloy at 298K.

x_{Na}	$\Delta H_{\text{Na-Pb}}$ /(kJ·mol^{-1})	$\Delta S^{E}_{\text{Na-Pb}}$ /(J·mol^{-1}·K^{-1})	$\Delta G^{E}_{\text{Na-Pb}}$ /(kJ·mol^{-1})	γ_{Na}	γ_{Pb}
0.1	−8	−2	−7	0.0000	0.7888
0.2	−15	−5	−14	0.0000	0.3391
0.3	−22	−7	−20	0.0000	0.0653
0.4	−27	−8	−24	0.0000	0.0053
0.5	−28	−9	−25	0.0000	0.0002
0.6	−25	−8	−23	0.0007	0.0000
0.7	−20	−6	−18	0.0233	0.0000
0.8	−13	−4	−12	0.2279	0.0000
0.9	−7	−2	−6	0.7246	0.0000

Table S4. Calculated values of $\Delta H_{\text{Na-Sn}}$, $\Delta S^{E}_{\text{Na-Sn}}$, $\Delta G^{E}_{\text{Na-Sn}}$, γ_{Na} and γ_{Sn} of Na-Sn alloy at 298K.

x_{Na}	$\Delta H_{\text{Na,Sn}}$ /(kJ·mol^{-1})	$\Delta S^{E}_{\text{Na,Sn}}$ /(J·mol^{-1}·K^{-1})	$\Delta G^{E}_{\text{Na,Sn}}$ /(kJ·mol^{-1})	γ_{Na}	γ_{Sn}
0.1	−4	−1	−3	0.0000	0.8859
0.2	−8	−3	−7	0.0000	0.5796
0.3	−11	−4	−10	0.0000	0.2577
0.4	−13	−4	−12	0.0003	0.0775
0.5	−13	−4	−12	0.0039	0.0174
0.6	−12	−4	−11	0.0350	0.0035
0.7	−9	−3	−8	0.1818	0.0008
0.8	−6	−2	−6	0.5146	0.0002
0.9	−3	−1	−3	0.8664	0.0001

Table S5. Calculated values of $\Delta H_{\text{Na-Cu}}$, $\Delta S^{E}_{\text{Na-Cu}}$, $\Delta G^{E}_{\text{Na-Cu}}$, γ_{Na} and γ_{Cu} of Na-Cu alloy at 298K.

x_{Na}	$\Delta H_{\text{Na-Cu}}$ /(kJ·mol^{-1})	$\Delta S^{E}_{\text{Na-Cu}}$ /(J·mol^{-1}·K^{-1})	$\Delta G^{E}_{\text{Na-Cu}}$ /(kJ·mol^{-1})
0.1	+10	+2	+9
0.2	+19	+5	+18
0.3	+24	+6	+22
0.4	+25	+6	+23
0.5	+23	+6	+21
0.6	+19	+5	+17
0.7	+14	+3	+13
0.8	+9	+2	+9
0.9	+5	+1	+4

Table S6. Calculated values of $\Delta H_{\text{Na-Cr}}$, $\Delta S^{E}_{\text{Na-Cr}}$, $\Delta G^{E}_{\text{Na-Cr}}$, γ_{Na} and γ_{Cr} of Na-Cr alloy at 298K.

x_{Na}	$\Delta H_{\text{Na-Cr}}$ /(kJ·mol^{-1})	$\Delta S^{E}_{\text{Na-Cr}}$ /(J·mol^{-1}·K^{-1})	$\Delta G^{E}_{\text{Na-Cr}}$ /(kJ·mol^{-1})
0.1	+44	+10	+41
0.2	+85	+19	+80
0.3	+109	+25	+102
0.4	+112	+25	+105
0.5	+102	+23	+95
0.6	+84	+19	+78
0.7	+63	+14	+59
0.8	+42	+9	+39
0.9	+21	+5	+20

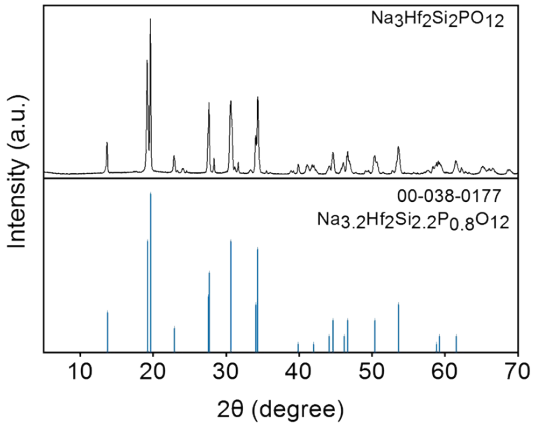

Figure S1. XRD characterization of $Na_3Hf_2Si_2PO_{12}$ pellet.

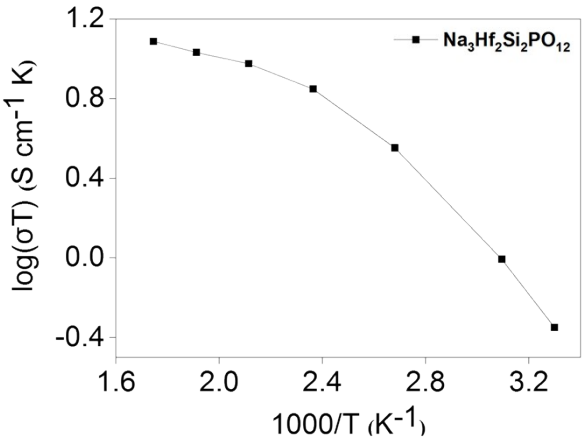

Figure S2. The Arrhenius plot of $Na_3Hf_2Si_2PO_{12}$.

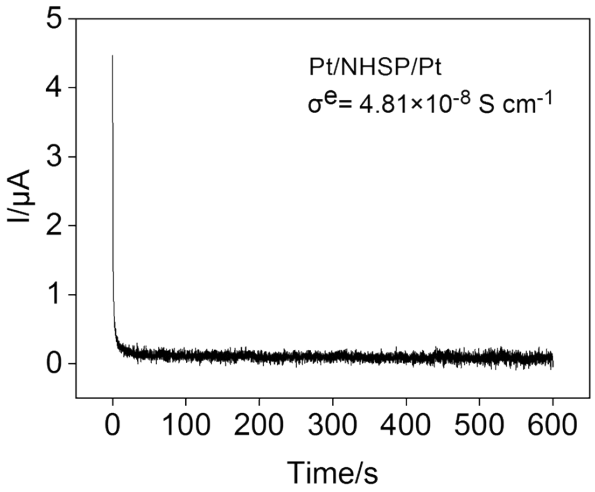

Figure S3. DC polarization curve of $Na_3Hf_2Si_2PO_{12}$ at 30 °C.

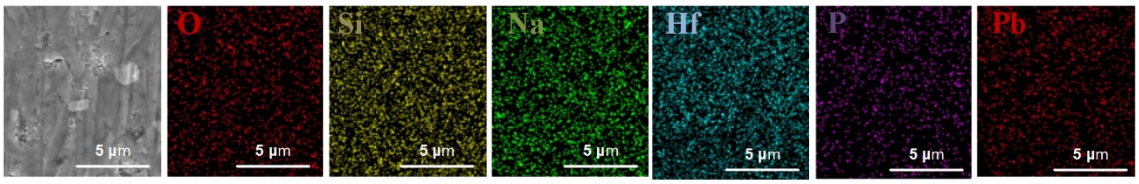

Figure S4. Top view SEM image of $Na_3Hf_2Si_2PO_{12}$ with Pb coating, and EDS maps of O, Si, Na, Hf, P, Pb.

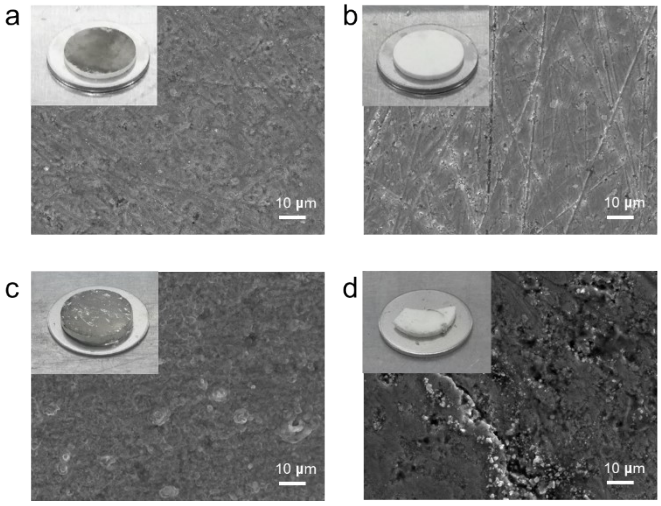

Figure S5. SEM images of $Na_3Hf_2Si_2PO_{12}$ surface before cycling (a) with Pb coating, and (b) without Pb coating. SEM images of NHSP surface after cycling. (c) with Pb coating, and (d) without Pb coating.

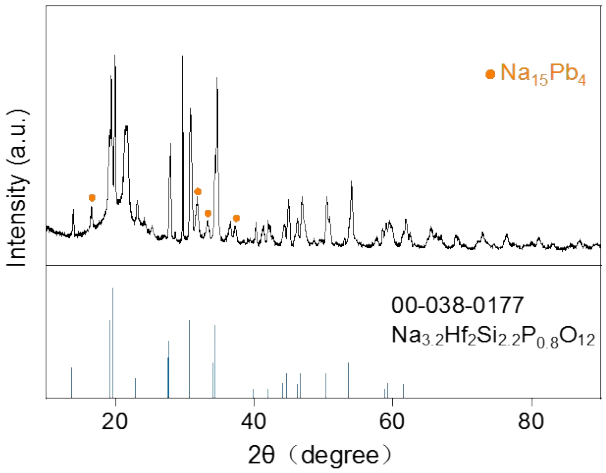

Figure S6. XRD of the $Na_3Hf_2Si_2PO_{12}$ electrolyte surface after cycling.

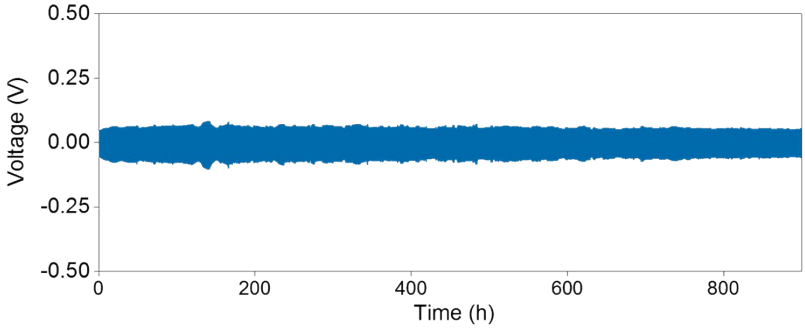

Figure S7. The symmetric batteries of Na|Pb-$Na_3Hf_2Si_2PO_{12}$-Pb|Na at 0.2 mA cm^{-2} at room temperature.

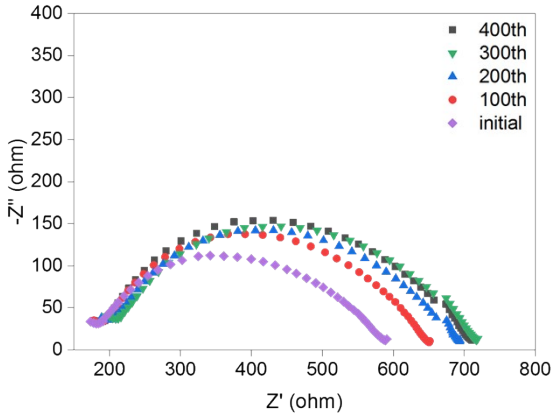

Figure S8. Nyquist plots of the Na|Pb-$Na_3Hf_2Si_2PO_{12}$-Pb|Na symmetric battery after cycling for different times.

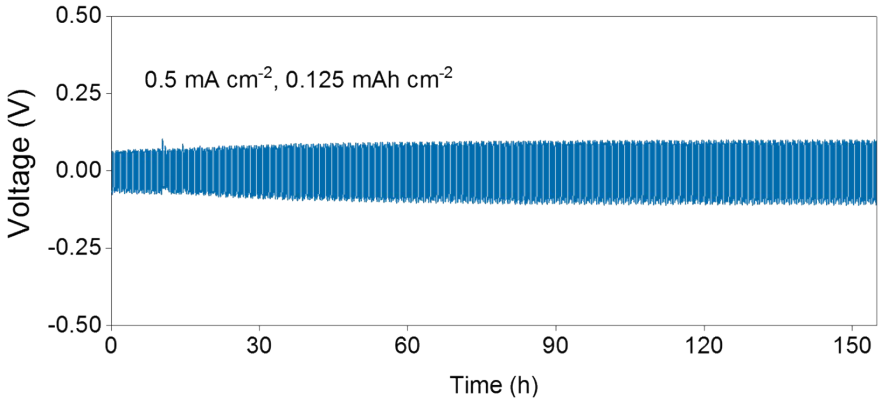

Figure S9. The symmetric batteries of Na|Pb-$Na_3Hf_2Si_2PO_{12}$-Pb|Na at 0.5 mA cm^{-2} at 60 °C.

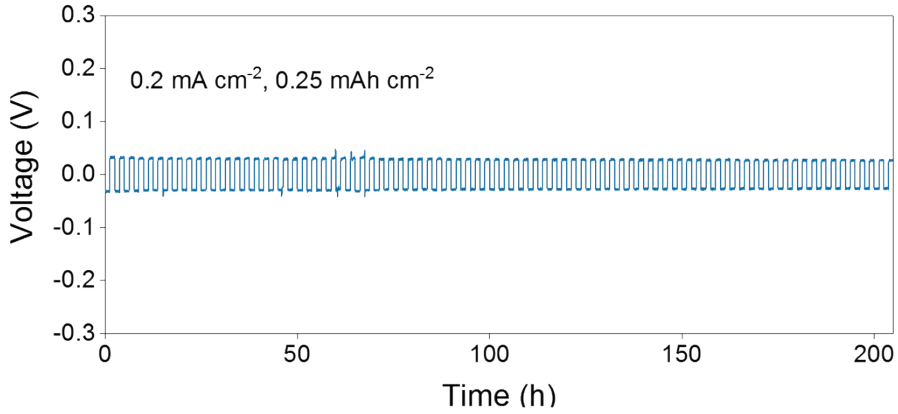

Figure S10. The symmetric batteries of Na|Pb-$Na_3Hf_2Si_2PO_{12}$-Pb|Na at 0.2 mA cm^{-2} at 60 °C.

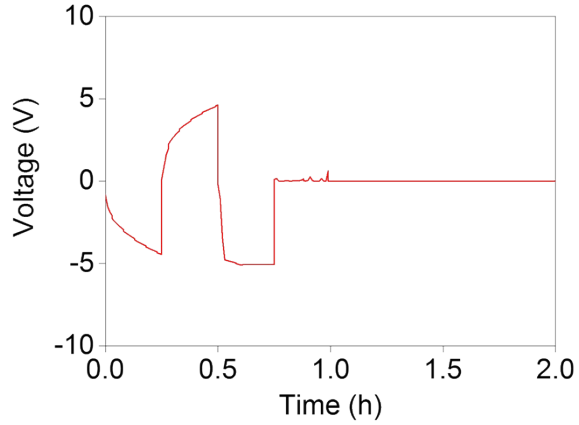

Figure S11. Galvanostatic cycling performance of the Na|$Na_3Hf_2Si_2PO_{12}$|Na symmetric battery at 0.05 mA cm^{-2} at room temperature.

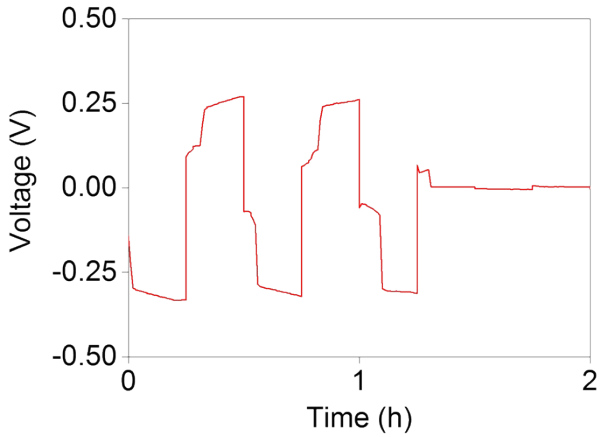

Figure S12. Galvanostatic cycling performance of the Na|$Na_3Hf_2Si_2PO_{12}$|Na symmetric battery at 0.1 mA cm^{-2} at 60 °C.

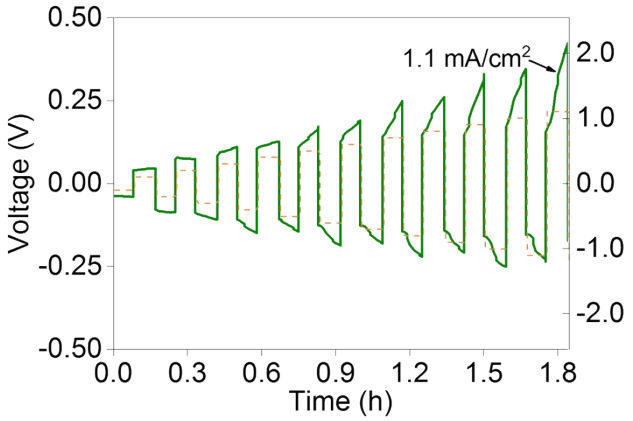

Figure S13. Critical current density test of the Na|Cu-$Na_3Hf_2Si_2PO_{12}$-Cu|Na symmetric battery at 60 °C.

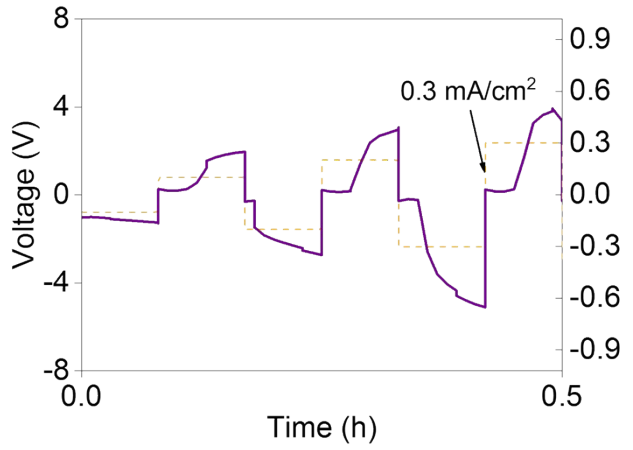

Figure S14. Critical current density test of the Na|Cr-$Na_3Hf_2Si_2PO_{12}$-Cr|Na symmetric battery at 60 °C.

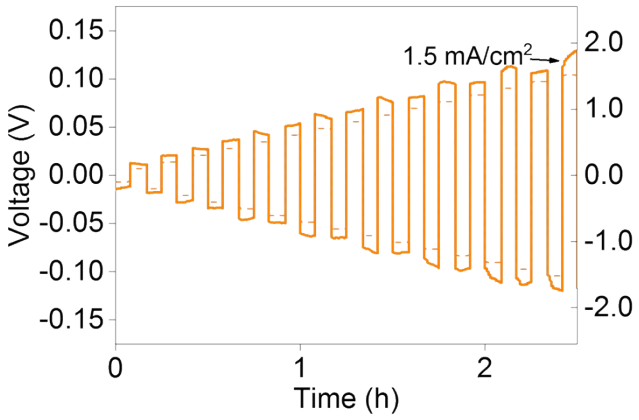

Figure S15. Critical current density test of the Na|Sn-$Na_3Hf_2Si_2PO_{12}$-Sn|Na symmetric battery at 60 °C.

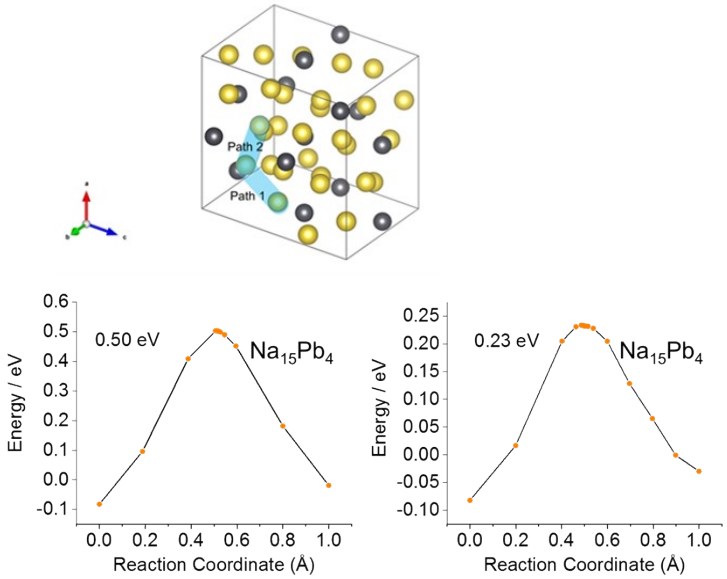

Figure S16. The crystal structure, diffusion path and diffusion energy barrier of Na^+ in $Na_{15}Pb_4$.

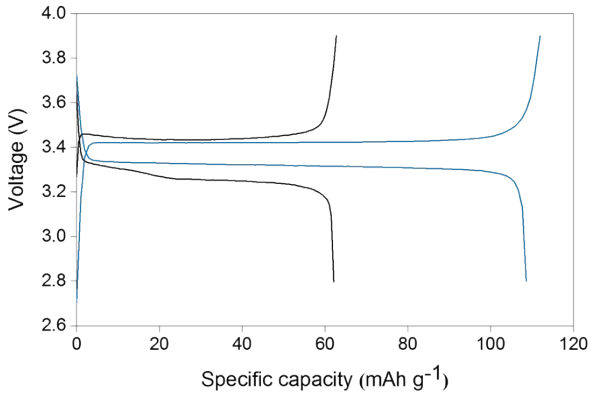

Figure S17. Discharge capacity of the full cell with and without Pb coating in the first cycle, the blue one is with Pb coating and the black one is without Pb coating.

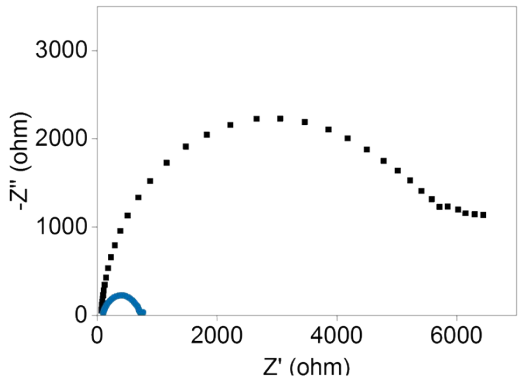

Figure S18. The EIS profiles of the full cells with and without lead coated NHSP, the blue one is with Pb coating and the black one is without Pb coating.

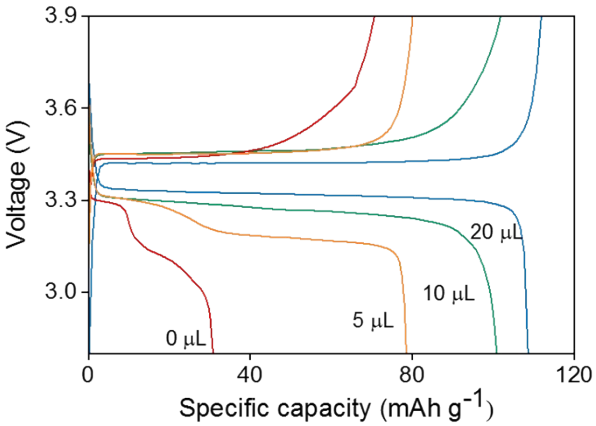

Figure S19. Charge-discharge curves of the full cell with different amount of liquid electrolyte in the first cycle under a current density of 0.5 C.

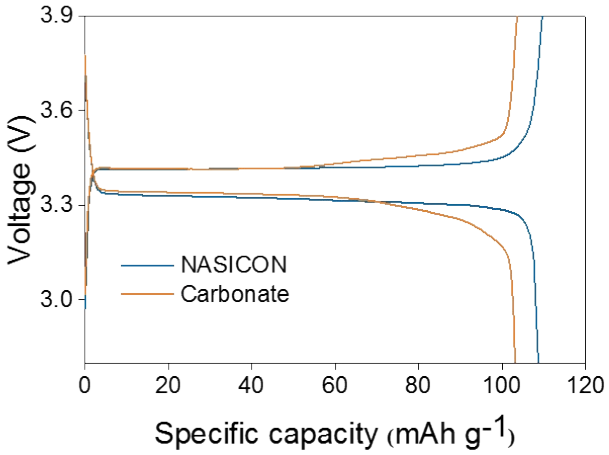

Figure S20. Charge and discharge curves of the full cell with and without carbonate liquid electrolyte under a current density of 0.5 C.

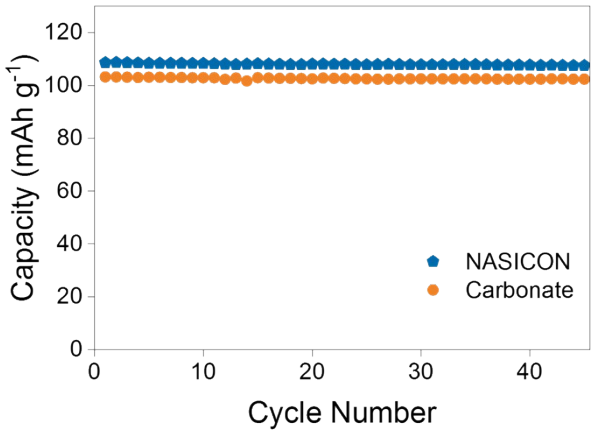

Figure S21. The cycling performance of the full cell with and without carbonate liquid electrolyte under a current density of 0.5 C.

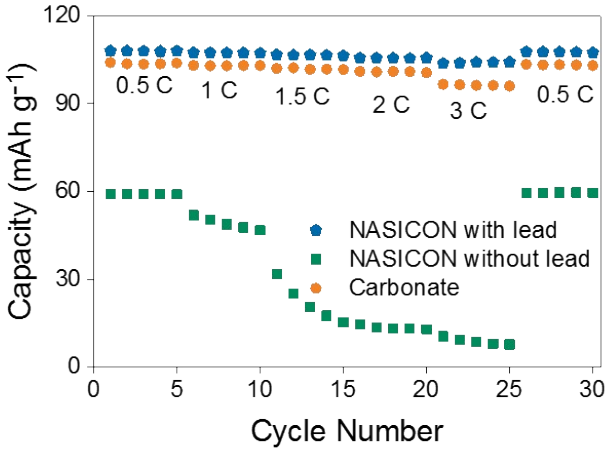

Figure S22. The rate performance of the full cell with and without liquid electrolyte.

Table S7. Recent advances in long-cycle symmetric cells based on NASICON-type electrolytes.

Battery type	Critical current density (mA cm^{-2})	Stability (mA cm^{-2} /cycles)	Test temperature	Ref.
Na-TiO_2-NASICON	N	0.1/860	RT	2
Na-SiO_2-NASICON	0.5	0.1-0.2/135	RT	3
Na-AlF_3-NASICON	1.2	0.15-0.25/300	60 °C	4
Na-CPMEA-NASICON	N	0.2/380	65°C	5
Na-Pb-NASICON	2.5	0.1/2450	RT	This work
		0.2/900	RT	
		0.5/150	60 °C	

Table S8. Recent advances in the electrochemical performance of full cells based on $Na_3V_2(PO4)_3$ cathodes and NASICON-type electrolytes.

Battery type	Stability (C /cycles)	Current density	Test temperature	Ref
Na-TiO_2-NASICON	0.1 C/60	N	60 °C	2
Na-SiO_2-NASICON	N	N	N	3
Na-AlF_3-NASICON	1 C/100	N	RT	4
Na-CPMEA-NASICON	0.2 C/70	N	65 °C	5
Na-Pb-NASICON	0.5 C/150	3 C	RT	This work

Notes and References

[1] K. Mathew, R. Sundararaman, K. Letchworth-Weaver, T. A. Arias, R. G. Hennig, *J. Chem. Phys.*, 2014, **140**, 084106.

[2] J. Yang, Z. Gao, T. Ferber, H. Zhang, C. Guhl, L. Yang, Y. Li, Z. Deng, P. Liu, C. Cheng, R. Che, W. Jaegermann, René Hausbrand, Y. Huang, *J. Mater. Chem. A*, 2020, **8**, 7828.

[3] H. Fu, Q. Yin, Y. Huang, H. Sun, Y. Chen, R. Zhang, Q. Yu, L. Gu, W. Luo, *ACS Mater. Lett.*, 2019, **2**, 127.

[4] X. Miao, H. Di, X. Ge, D. Zhao, P. Wang, R. Wang, C. Wang, L. Yin, *Energy Storage Mater.*, 2020, **30**, 170.

[5] W. Zhou, Y. Li, S. Xin, J. B. Goodenough, *ACS Cent. Sci.*, 2017, **3**, 52.